Bogdan SAPIŃSKI*, Łukasz JASTRZĘBSKI*

LABORATORY SETUP FOR TESTING THE MODELS OF MR SUSPENSIONS WITH ENERGY RECOVERY CAPABILITY

SUMMARY

The paper presents the experimental set-up for laboratory testing of MR damper-based suspension systems. The model and structure of a suspension system with energy recovering, measurement-control system of the set-up and results of functional tests are described. Transmissibility plots and time patterns of the suspension characteristic quantities are determined.

Keywords*: suspension, MR damper, generator, vibration, energy recovering*

STANOWISKO DO BADAŃ MODELI ZAWIESZEŃ MAGNETOREOLOGICZNYCH Z ODZYSKIEM ENERGII

W pracy przedstawiono stanowisko do badań laboratoryjnych modeli zawieszeń magnetoreologicznych (MR). Opisano model i budowę zawieszenia z odzyskiem energii, układ pomiarowo-sterujący stanowiska oraz wyniki jego testów funkcjonalnych. Wyznaczono charakterystyki przenoszenia drgań i przebiegi czasowe wielkości charakteryzujących działanie zawieszenia.

Słowa kluczowe*: zawieszenie, tłumik MR, generator, drgania, odzyskiwanie energii*

1. INTRODUCTION

The issues relating to energy recovery from the surroundings and its use in power-supply systems have received a great deal of attention in the last decade (Prima, Innan 2009). As regards the recovery of mechanical energy of vibrations, the research efforts focus mostly on seeking alternative solutions to conventional small-power energy sources.

This study explores the applications of an electromagnetic technique of mechanical-to-electric energy conversion in semiactive suspensions incorporating MR dampers. The physical model of the suspension comprises commercially available MR dampers and a prototype electromagnetic generator (Sapiński 2010). The laboratory setup is outlined and experimental data are provided.

2. MR SUSPENSION MODEL

The model of the suspension is shown schematically in Figure 1. The suspension and the vibro-isolated object represent a two degree-of-freedom system. The energy regenerative vibration reduction system include a suspension plate with the mass m_1, a spring 1 with the stiffness k_1, a MR damper 1 and an electromagnetic generator G which converts the energy of vibration into electric energy power-supplying the control coil in a MR damper 1, thus providing the energy recovery capability. The upper part of the suspension model, to which the vibro-isolated object with the mass m_2 is attached, incorporates a spring 2 with the stiffness k_2 and a damper MR 2.

Displacements of the suspension plate x_1 and of the object to be vibro-isolated are induced by kinematic excitations (displacement z). Forces F_1 and F_2 generated by the dampers MR 1 and 2 are associated both with the piston velocity with respect to the cylinder and with currents i_1, i_2 in the control coils in these dampers. Coefficients c_1 and c_2 represent viscous damping of the dampers MR 1 and 2 while their coils are supplied with direct current. The general view of the suspension model is shown in Figure 2. The model incorporates two MR dampers of the type RD-1005-3 Lord Corporation (Lord Co. 2011) mounted axially, inside the springs. Between the shaker plate and the suspension plate is the generator. Its axis of symmetry is shifted with respect to that of the suspension. That is why the vibration reduction system is provided with extra guides with linear

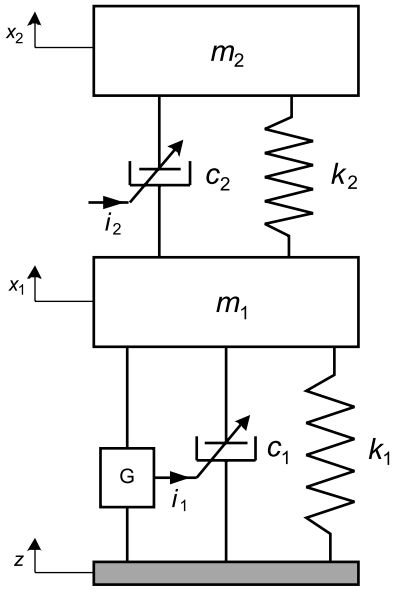

Fig. 1. Schematic diagram of the suspension model

* AGH University of Science and Technology, Faculty of Mechanical Engineering and Robotics, al. A. Mickiewicza 30, 30-059 Krakow, Poland; deep@agh.edu.pl; lukasz.jastrzebski83@gmail.com

bearings (Fig. 2), the suspension plate is attached to the main frame via two guides with linear bearings in order to eliminate the disturbances of the axial motion of the suspension model.

MR dampers allow the control of the damping force in each DOF separately. The control coil in the damper MR 1 can be supplied from the generator G (an energy-regenerative vibration reduction system) or from an external source of energy. The damping in the second DOF is regulated by setting the constant current level i_2 in the control coil of the damper MR 2 supplied from an external source.

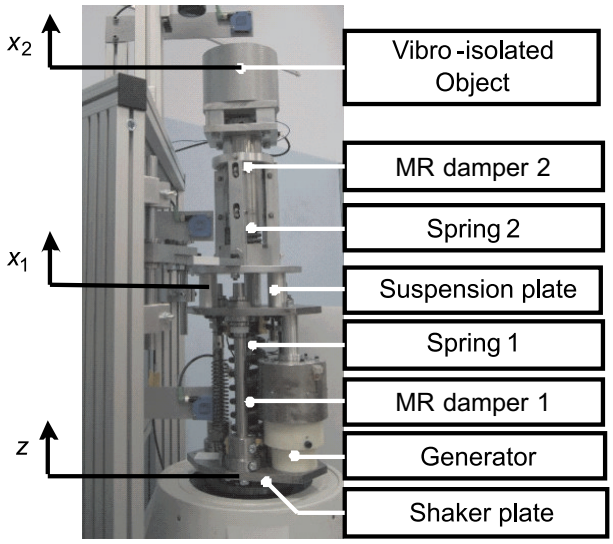

Fig. 2. Suspension model – general view

Parameters in the suspension model are based on the following assumptions:

- maximal mass of the system attached to the shaker: 70 kg,
- maximal amplitude of the applied excitations: 6 mm,
- the converter generates the required voltage to effectively power-supply the damper MR 1 at the velocity < 0.1 m/s,
- rms value of the MR 1 damper force for the piston velocity 0.2 m/s when the control coil is supplied from the generator: 460 N,
- rms value of the MR 1 damper force for the piston velocity 0.2 m/s and the control coil not supplied: 100 N,
- natural frequency of vibrations of the suspension model: 3.25 Hz and 11.25 Hz.

The suspension model performance is first simulated numerically in the MATLAB environment. Parameters in the simulation procedure are compiled in Table 1. The friction forces in the guiding system (linear bearings) are neglected. The applied sine excitations have the amplitude 3.5 mm and frequency in the range (2, 16) Hz.

Table 1

Parameters of the suspension model

Parameter	Values	
m_1	24	kg
m_2	35	kg
k_1	100000	N/m
k_2	18000	N/m
c_1	500	Ns/m
c_2	500	Ns/m

Simulation results in the form of transmissibility plots T_{x1z} and T_{x2z} are shown in Figure 3, revealing resonance frequencies of the suspension model: f_{r1}= 3.3 Hz and f_{r2}= 9.9 Hz.

3. EXPERIMENTAL SETUP

The experimental setup is shown schematically in Figure 4, comprising the system generating mechanical vibrations and the measurement and control system. The key component of the vibration generation system is an electromagnetic shaker V780 (LDS) interacting with the power amplifier HPA-K (Bruel & Kjaer 2011). The shaker is equipped with a compressor to compensate for the weight of the suspension on the shaker plate. The shaker performance is controlled by the Dactron Laser USB controller (Bruel & Kjaer

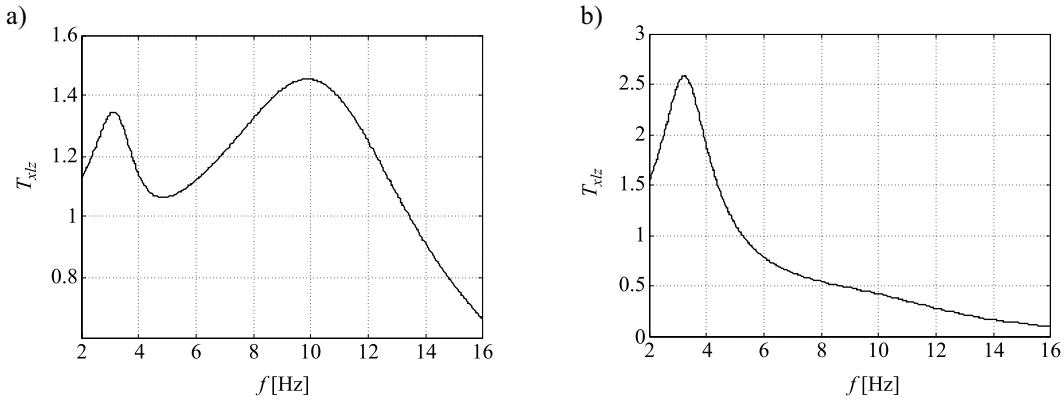

Fig. 3. Computed transmissibility values: a) T_{x1z}; b) T_{x2z}

2011) equipped with a piezoelectric accelerometer 357B33 PCB Pieztronics (PCB Pieztronics 2011) placed on the shaker plate. The controller communicates via a USB port with the computer with the dedicated software Dactron Shaker Control.

The measurement and control system has the capability to register the excitations z and displacements x_1, x_2 (laser sensors FT 50 RLA 70 (SensoPart 2011)), force F_1 (strain sensor EMS 30 EMSYST (Emsyst 2011) interacting with an amplifier) and force F_2 (piezoelectric sensors 208-C03 PCB Pieztronics) with a signal conditioner 480B21 (PCB Piezotronics 2011), current intensity i_1 in the control coil of the MR 1 damper and the voltage in the generator u. These quantities are converted into voltage signals in the range (–10, +10) V and processed by the I/O AC/CA card of the type RT-DAC Inteco (Inteco 2011) interacting with the MATLAB/Simulink environment. The experimental setup is shown in Figure 5.

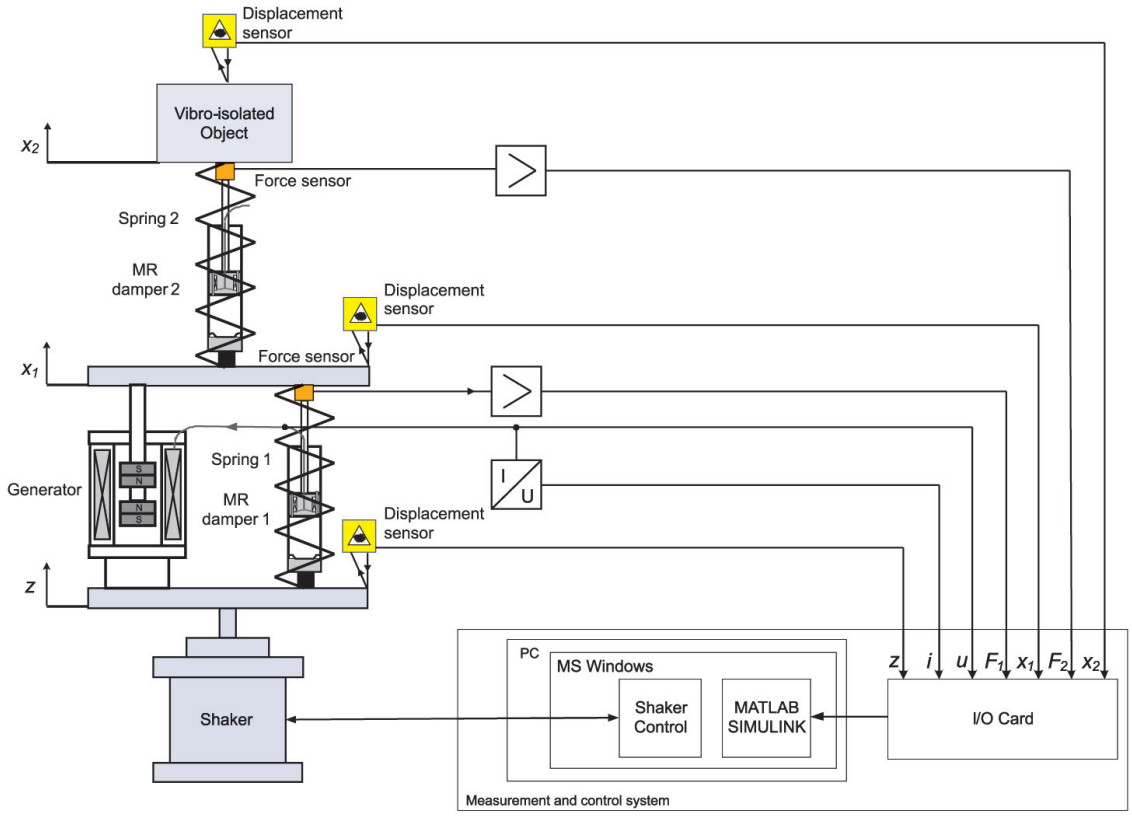

Fig. 4. Schematic diagram of the experimental setup

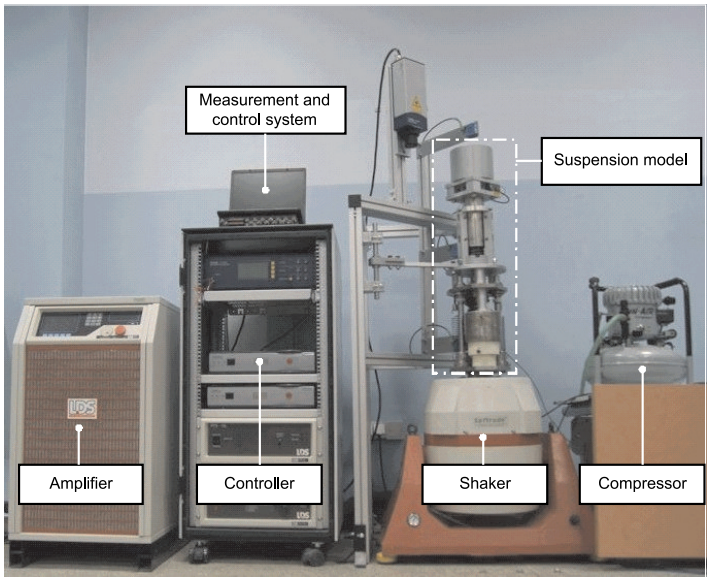

Fig. 5. Experimental setup-general view

4. PERFORMANCE TESTS

Performance tests are performed under the clearly defined conditions: when the control coil in the damper MR1 is not supplied at all (i_1 = 0 A) or when it is supplied from the generator with current in the control coil of the damper MR 2: I_2 = 0A, I_2 = 0.1 A, I_2 = 0.2 A. For clarity, the designations given in Table 2 are introduced to facilitate the analysis of test results. The applied sine excitations have the amplitude 3.5 mm whilst the frequency is linearly increasing from 2 to 16 Hz within the time period 240 s.

Table 2

Power supply to the coils – options

	No power-supply to the MR 1 damper	Damper MR 1 supplied from the generator
I_2 = 0 A	UP1	US1
I_2 = 0.1 A	UP2	US2
I_2 = 0.2 A	UP3	US3

Selected results of performance tests are shown in Figs. 6–12. Transmissibility plots T_{x1z} and T_{x2z} shown in Figures 6 and 7 are derived from the formulas:

$$T_{x_1z}(f_k)=\frac{|X_1(f_k)|}{|Z(f_k)|},\quad T_{x_2z}(f_k)=\frac{|X_2(f_k)|}{|Z(f_k)|} \tag{1}$$

$$0 \le k \le N-1$$

where: $Z(f_k)$, $X_1(f_k)$, $X_2(f_k)$ are discrete Fourier transforms (DFT) of the registered displacement signals z, x_1, x_2 for the frequency $f_k = k{\cdot}\Delta f$, k – frequency index, N – number of samples, Δf – frequency increment.

The plot of transmissibility T_{x1z} in the system UP1 (Fig. 6a) reveals the resonance frequencies of the suspension model: f_{r1}=3.5 Hz and f_{r2}= 8.3 Hz. These values f_{r1} and f_{r2} differ from those obtained from numerical simulations (Fig. 3) by 7% and 20%, respectively. The differences in

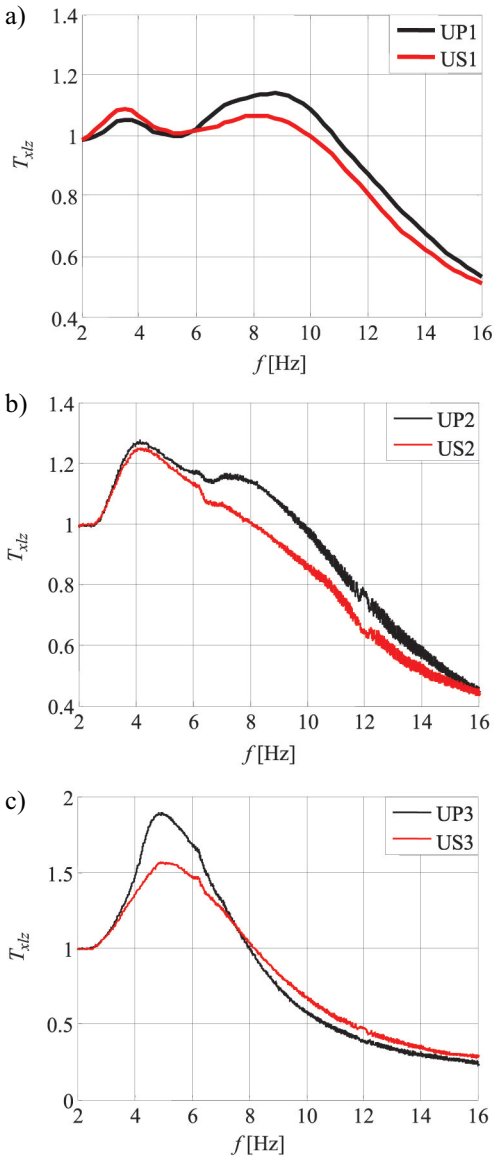

Fig. 6. Transmissibility T_{x1z}:
a) I_2 = 0 A; b) I_2 = 0.1 A; c) I_2 = 0.2 A

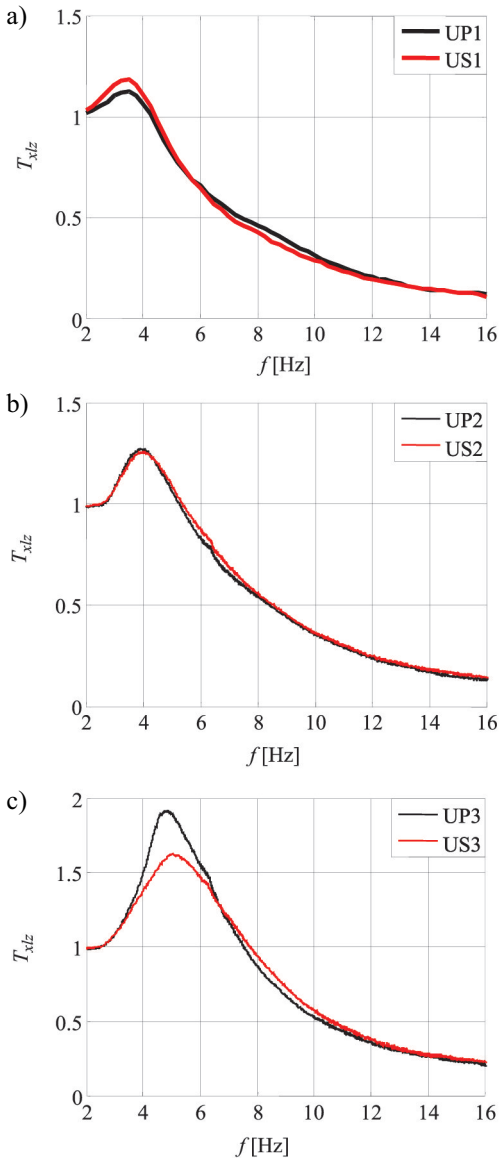

Fig. 7. Transmissibility T_{x2z}:
a) I_2=0 A; b) I_2=0.1 A; c) I_2=0.2 A

transmissibility levels T_{x1z} and T_{x2z} obtained experimentally may be caused by the fact that friction forces and nonlinearities of the damper force MR are neglected Comparison of transmissibility plots T_{x1z} for passive systems UP1, UP2, UP3 (Fig. 6a–c) reveals that increasing the MR2 damper force leads to an increased level of f_{r1}, at the same time the value of f_{r2} goes down. The plot of transmissibility T_{x1z} (Fig. 6c) shows that for the current in the control coil $I_2 = 0.2$ A we get one maximum for the frequency $f_r = 4.9$ Hz. The transmissibility plot T_{x2z} in Figure 7 reveals the occurrence of the resonance frequency f_{r1} in the systems UP1, UP2, UP3.

Comparison of transmissibility plots T_{x1z} for the systems US1, US2, US3 (where the generator supplies the control coil in the damper MR 1) and for UP1, UP2, UP3 reveals that its value decreases by more than ten percent for the frequency f_{r2}. In the energy regenerative system the value of transmissibility T_{x1z} at the resonance frequency will not decrease on account of low voltage produced by the generator due to small relative velocity of the suspension plate with respect to the shaker plate. The similar effect is observed in the case of transmissibility T_{x2z}.

Figures 8–12 show the time patterns of displacements x_1, x_2, voltage u, current intensity i_1 and forces F_1, F_2 for the systems UP1 and US1, registered at the frequency $f_{r1} = 3.5$ Hz and $f_{r2} = 8$ Hz. Increasing the frequency of the applied excitation z results in increase a phase shift of the displacements x_1, x_2 with respect to the applied excitation z (Figs. 8, 9). For the frequency f_{r2} the displacement amplitude x_1 in the system US1 (Fig. 9b) tends to decrease in relation to the value registered for the system UP1 (Fig. 8b).

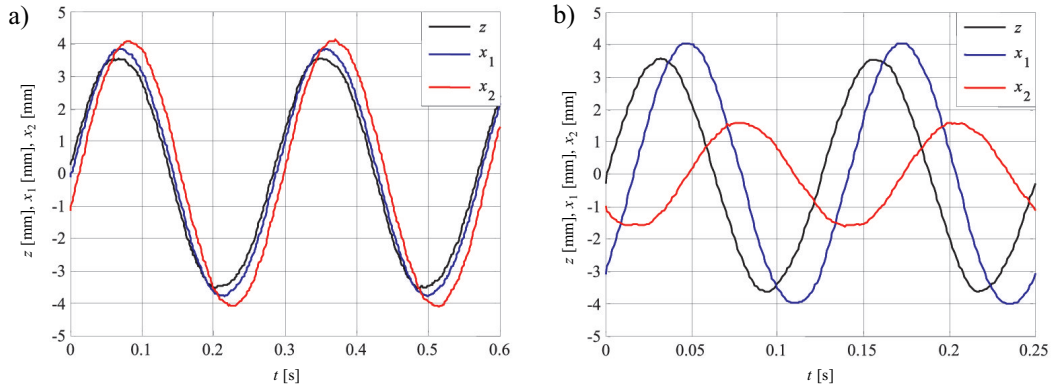

Fig. 8. Displacements x_1, x_2 vs time in the system UP1 under the applied excitation z with the frequency: a) 3.5 Hz; b) 8 Hz

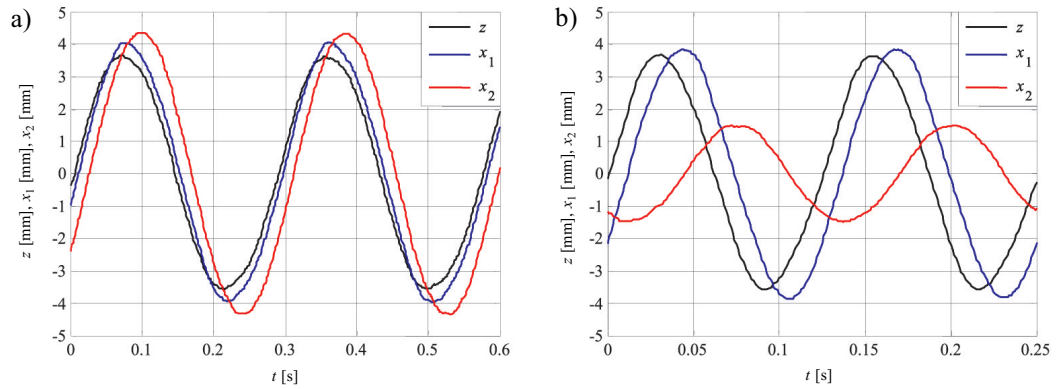

Fig. 9. Displacements x_1, x_2 vs time in the system US1 under the applied excitation z with the frequency: a) 3.5 Hz; b) 8 Hz

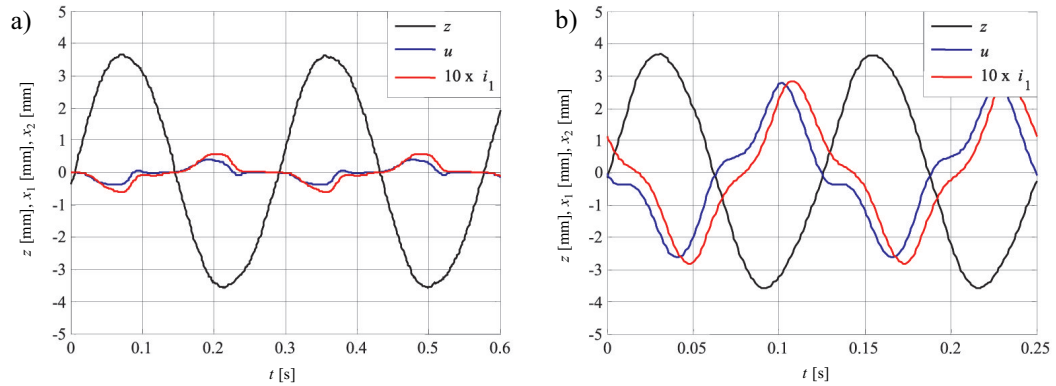

Fig. 10. Voltage u and current intensity i vs time in the system US1 under the applied excitation z with the frequency: a) 3.5 Hz; b) 8 Hz

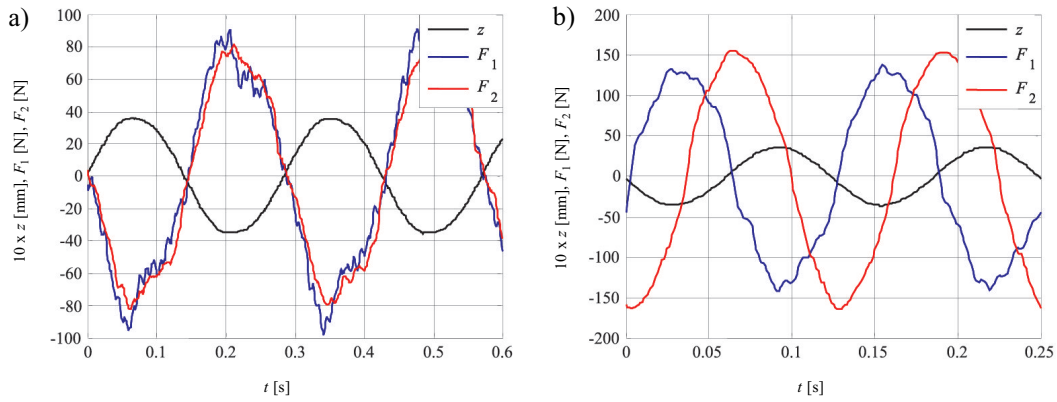

Fig. 11. Time patterns of forces F_1, F_2 in the system UP1 under the applied excitation z with the frequency: a) 3.5 Hz; b) 8 Hz

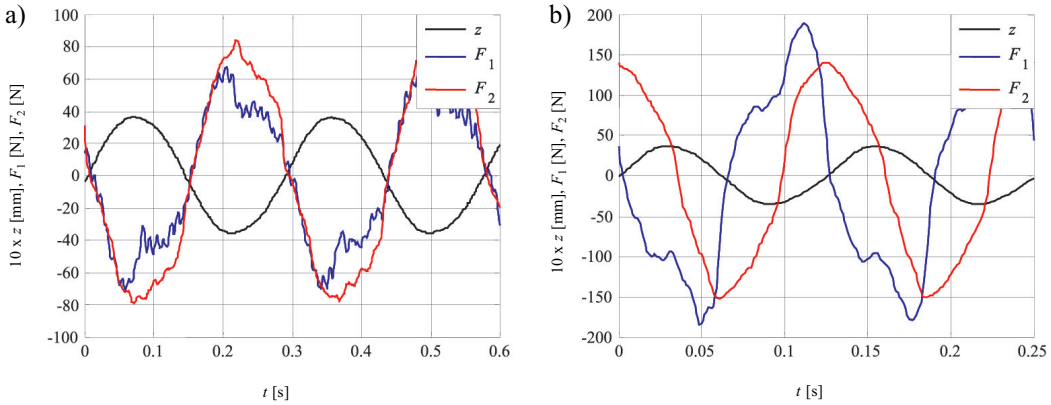

Fig. 12. Time patterns of forces F_1, F_2 in the system US1 under the applied excitation z with the frequency: a) 3.5 Hz; b) 8 Hz

Time patterns of voltage u generated by the generator and of current i are shown in Figure 10. These patterns are deformed. For the frequency f_{r1}, the amplitude of voltage u does not exceed 0.4 V, inducing the current flow in the control coil of the damper MR 1 of the maximal value 0.05 A. This is insufficient to considerably increase the damping force generated by the damper MR 1. For the frequency f_{r2}, the value of voltage u and current i are larger (their respective amplitudes being 2.87 V and 0.3 A). The phase shift between the current i and voltage u is attributable to the fact that the loading imposed by the damper coil upon the generator is of the resistance and inductive type. In the case of the damper MR 1, supplying the coil from the generator (US1) causes that for the frequency f_{r1} (Fig. 12a) the maximal damping force F_1 will decrease in relation to the passive system UP1 (Fig. 11a) whilst for the frequency f_{r2} (Fig. 12b) the damper supplied from the generator (US1) generates a larger damping force than in the passive system UP1 (Fig. 11b).

Deformations of the force patterns F_1, F_2 are attributable to nonlinearities associated with the hysteresis loop in MR dampers (Sapiński 2006).

5. SUMMARY

In this study the physical model of a energy regenerative magnetorheological suspension is presented, the test facilities are described and the performance test data are summarised. The operating principles of the suspension are explained, the parameters of the suspension model are given and numerical data obtained from simulation are provided. The mechanical structure of the setup and the measurement and control system are described, followed by selected test data.

Basing on the registered displacement signals z, x_1, x_2, the transmissibility factors T_{x1z}, T_{x2z} of the suspension model are derived. Resonance frequencies of the suspension models are very close to predicted values obtained in numerical simulations. Time patterns are duly derived of generated voltage and current intensity in the control coil of the damper MR 1 under the applied excitation z at resonance frequencies. The suspension model is shown to display the self-supplying capability, leading to reduction of the transmissibility coefficient T_{x1z} at the resonance frequency f_{r2} in comparison to the passive system.

This study is sponsored through the research grant no N501 366934.

References

Bruel & Kjaer, 2011, http://www.bksv.com.
Emsyst, 2011, http://www.emsyst.sk/.
Inteco, 2011, http://www.inteco.com.pl.
Lord Co., 2011, http://www.lord.com.
PCBPiezotronics, 2011, http://www.pcb.com.
SensoPart, 2011, http://www.sensopart.com.
Priya S., Inman D. (Eds.) 2009, *Energy harvesting Technologies*. Springer Science+Business Media.
Sapiński B. 2006, *Magnetorheological Dampers in Vibration Control*. AGH University of Science and Technology Press, Cracow.
Sapiński B. 2010, *Vibration power generator for a linear MR damper*. Smart Materials and Structures, vol. 19, 1050–10562.